CrossMark

ORIGINAL PAPER

Polypyrrole/copper nanoparticles composite thin films for high-sensing performance

V. B. Mamlayya[1] · **V. J. Fulari**[1]

Abstract In the present paper, we report the synthesis and application of poly-pyrrole thin films decorated by copper nanoparticles for the glucose detection. The PPy films were grown via, electrodeposition technique on stainless steel substrate. The structural study was carried out by X-ray diffraction study. The morphological study from field-emission-scanning electron microscopy depicted that decoration of copper nanoparticles over the polypyrrole thin film. The electroactivity of PPy/copper oxide/stainless steel electrode was explored using cyclic voltammetric study and chronoamperometry under pH $= 7 \pm 5$. The optimum sensitivity of optimized second electrode PPy/is 100 $\mu A\ mM^{-1}\ cm^{-2}$ with LOD 3 μM and regression coefficient $R^2 = 0.9951$. The PPy/copper-oxide sensor exhibited remarkable stability and reproducibility with good non-enzymatic current sensitivity.

Keywords Polypyrrole · Copper oxide · Glucose · Non-enzymatic sensor

Introduction

Many people around the world are suffering from diabetes which is a highly widespread disease bringing about metabolic disorders. Therefore, the blood glucose detection is very essential for diabetic patients and helps to evade the clustering of blood. Therefore, it is of high significance to establish straightforward

✉ V. J. Fulari
 vijayfulari@gmail.com

1   Holography and Material Research Laboratory, Department of Physics, Shivaji University, Kolhapur, MS 416004, India

system with high selectivity, sensitivity, and stability to distinguish glucose levels [1–3].

Conducting polymers offer a wide platform for chemical sensing and can be used as solid contact electrodes. They are more advantageous with good mechanical stability, simplicity, and possibility of miniaturization. Amongst different conducting polymers, polypyrrole (PPy) has many attractive features like ease of preparation, high stability, and amenability to use in neutral pH region. Furthermore, PPy exhibits electric conductivity and electrochemical redox activity [4]. Even in neutral pH solutions, which allow the entrapment of a wide range of biomolecules. Several authors have been reported enzyme-based biosensors by enzyme immobilization. Enzyme-based, i.e., glucose oxidase (GOD), Sing et al. reported reviews on PPy/GOD biosensors, shows enzyme specificity towards glucose, GOD enzyme immobilization techniques sensing performance of PPy/GOD. Xiao et al. reported that horseradish peroxidises/cysteamine modified gold electrode. The sensor displayed good electrocatalytic response to the reduction of H_2O_2 without the aid of an electron mediator [5]. Zhang et al. studied on gold nanoparticles modified hydrogen-peroxide sensor based on Hb [6]

Enzyme-based polymer was studied extensively. However, the enzymes were denatured readily and leached on the surface of electrode which leads during sensing mechanism is a major problem of enzyme-based sensors. To overcome this drawback, enzyme-free sensors are focused on the present context. PPy film could be further improved by embedding metal particles into the polymer matrix to form a metal–polymer composite [7, 8]. This polymer–metal nanocomposite can provide a highly porous structure with a large effective surface area, good electronic conductivity, and high catalytic activity [9]. Some metal–polymer nanocomposites have already been reported in the literature, such as PPy/Pt [10], PPy/Au [11], PPy/Ti [12], and PPy/Ag [13]. Moreover, Ozcan et al. [14] and Ozkorucuklu et al. [15] have reported molecularly imprinted polypyrrole and over oxidized PPy on pencil graphite electrodes for sensing of ascorbic acid and sulfamethaxazole, respectively. Another study by Wang et al. [16] reported the incorporation of copper (II) ions during adsorptive stripping voltammetric determination of tyrosine from pH 9.6 solutions by Liu et al. [17]. Liu et al. reported PPy encapsulated copper nanowires with excellent oxidation resistance and temporal stability [18]. Arvindan et al. studied anti-corrosion application of copper–polypyrrole [19]. Hea et al. observed enhancement in inductance of spiral copper [20]. Arena et al. reported non-enzymatic copper-oxide chitosan nanocomposite for hydrogen-peroxide sensor [21]. Sing et al. studied biosynthesis of copper nanoparticles using Shewanella loihica PV-4 with antibacterial activity [22]. Liang et al. reported electrochemical detection of hydrogen peroxide using copper nanoparticles in polyaniline film [23]. Kaviyarasan et al. studied sonochemically synthesized Cu_2O nanocubes for chemiluminescence application [24]

Polymer metals or metal-oxide composite is promising that functional materials show synergetic effect of both the materials. Various optical and electrochemical-sensing systems have been used for the detection of glucose [25–31]. Electrochemical systems are more attractive, mainly because of their simplicity, cost effectiveness, sensitivity, and selectivity [28, 32–34]. To offer selectivity towards

glucose, most of the electrochemical systems require glucose oxidase (GOx) that catalyzes b-D-glucose-to-glucono-D-lactone and H_2O_2 in the presence of O_2 [28, 32, 34, 35]. The as-produced glucono-D-lactone is subsequently converted to gluconic acid through hydrolysis. By monitoring the current generated from reduction of H_2O_2, the concentration of glucose can be determined [34]. Although these approaches are sensitive and selective, durability and short self-life of the electrodes are two other issues.

In the present study, amperometric sensors for glucose sensing are designed and developed via potentiostatic mode of electrodeposition on stainless steel. PPy/copper-oxide composite shows synergetic effect in the enhancement of sensing performance. PPy/copper-oxide composite films were used as non-enzymatic glucose sensor. Structural, morphological, and electrochemical studies were carried out using XRD, FE-SEM, and electrochemical studies. Copper-oxide-modified PPy electrode responds to glucose concentrations in the range 10–50 mM with a very low detection limit of 4 μM and by far the most sensitive one. Detailed cyclic voltammetric and chronoamperometric experiments were undertaken to investigate the electrocatalytic behaviour of glucose.

Experimental

Reagents

Pyrrole, dopamine, and uric acid were purchased from Sigma and used without further purification. Pyrrole (Py) was triply distilled until a colorless liquid was obtained and it was then stored under nitrogen before use. Sodium dodecylsulfate (SDS), $CuSO_4$, H_2SO_4, NaOH, and ethanol were of analytical-reagent grade and supplied from Sigma. All of the solutions were prepared using ultrapure water provided from an $18 \ M \ cm^{-1}$ Milli-Q system. All experiments were carried out at ambient temperature.

PPy/Cu NPs electrode preparation for non-enzymatic glucose sensor

The preparation of PPy/Cu NPs electrode completed in two steps. First, the PPy electrode is prepared using 0.2 M Py and 0.2 M H_2SO_4 electrodeposited at 0.65 V potential onto neatly polished and cleaned stainless steel substrate. Second, 0.1 M $CuSO_4$ solution prepared in double distilled water is decorated on the prepared PPy electrode for different cyclic voltammetries. As deposited PPy electrode is decorated by 5, 10, 15, and 20 cycles of $CuSO_4$ which are further termed the first, second, third, and fourth electrodes throughout the whole study of current work.

For detailed study of PPy/Cu NP electrodes, physicochemical studies were carried out. The structural characterization of PPy/Cu NPs is carried out by D2-Phraser Brukar model with Cu–Kɑ radiation operating at 40 kV and 15 mA. Surface morphology of PPy/Cu NPs nanostructure is studied by field-emission-scanning electron microscope (FE-SEM) of TESCAN. Electrochemical Analyzer/

Workstation used for electrochemical studies is of Model 600E Series for non-enzymatic glucose sensor of deposited PPy/Cu NP electrode.

## Results and discussion

X-ray diffraction study

Figure 1 shows the XRD pattern of PPy/Cu NPs films deposited on stainless steel substrates. The peak attributed to 43.5°, 50°, and 74° is of stainless steel rest peaks observed are of Cu nanoparticles. In addition, the peaks of Cu NPs are overlapped on the peaks of stainless steel substrate. It confirms the presence of copper nanoparticles particularly at 300 °C, which we attribute to a combination of partial crystallisation at lower temperatures and peak spreading caused by the nanoparticulate nature of the material [36]. On the other hand, Cu_2O deposited for different times, i.e., 10, 20, 30, and 40 s, respectively, exhibits the XRD patterns, as shown in Fig. 1b–e. Amongst all the diffractograms, prominent peaks are observed in Fig. 1c. Peaks observed in Fig. 1d, e go on reducing may be due to larger crystallite size of Cu_2O. No diffraction lines associated with impurities were detected in the present study. These XRD results match well with JCPDS 05-0667 with cubic fcc structure of Cu_2O representing (111), (200), and (220) planes. From XRD results, it can be explained the mechanism of reducing $CuSO_4$ with solution of NaOH and the reduction of Cu^{2+} ion in the solution to Cu^+ ion which is deposited as Cu_2O particles on PPy electrode [37].

Fig. 1 XRD patterns of PPy/Cu NPs films: bare stainless steel (**a**), first electrode (**b**), second electrode (**c**), third electrode (**d**), and fourth electrode (**e**), respectively
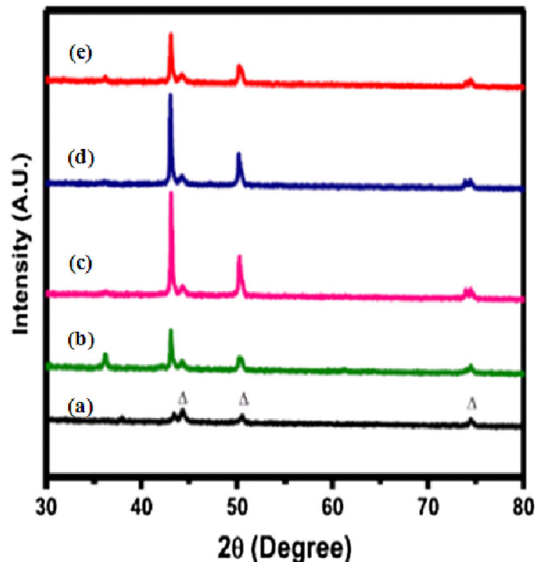
Surface morphological study

The morphology of PPy and PPy/Cu NPs films was investigated by FE-SEM shown in Fig. 2. Figure 2a shows that the irregular grain-like morphology of copper particles was dispersed randomly on PPy film for 10 s. In Fig. 2b, the agglomeration of grain-like structures forms cluster of copper nanoparticles which provide much space to copper nanoparticle to interact with glucose due to interconnecting leaf-like structure between the clusters, while Fig. 2c reflects the change in morphology in terms of size and shape of the particles and slowly become compact with loosing leaf-like structure between them. When time of deposition copper on PPy film increase morphology gradually changes and finally becomes flower like, as shown in Fig. 2d. This kind of morphology of PPy/Cu NPs shows comparatively less amperometric response than that of Fig. 2b second-type electrode. Figure 3 shows that the stiochiometry of PPy/Cu nanocomposite films is studied by EDS study analysis, as shown in Table 1. As no. of copper-oxide cycles on PPy film increases, an atomic percentage of Cu nanoparticles for the first and second black PPy films becomes blackish brown and Cu nanoparticles are dispersed uniformly on the PPy
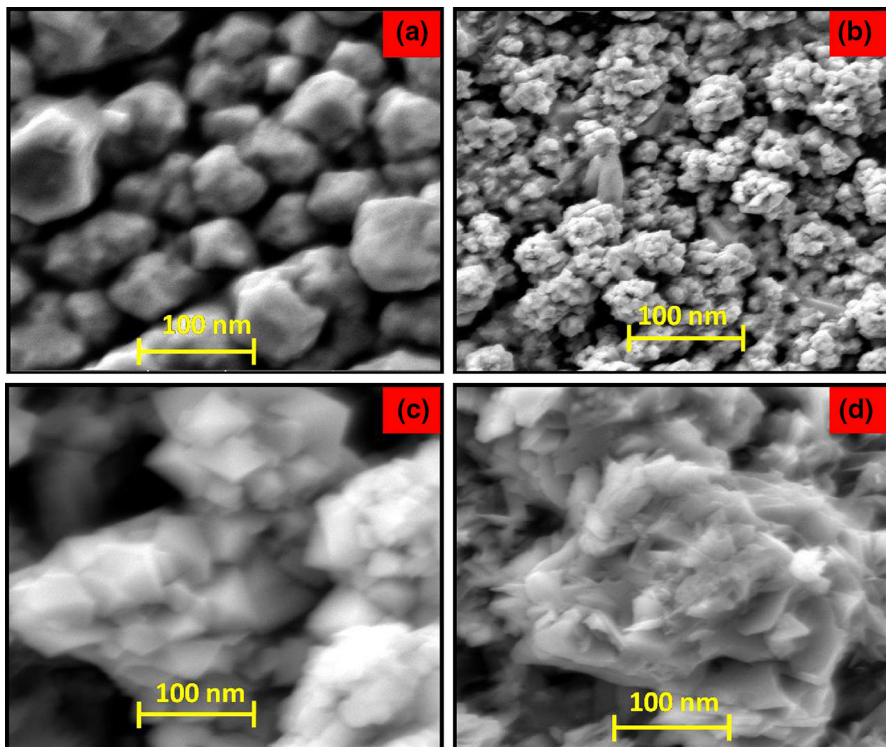
Fig. 2 Surface morphology of PPy/Cu NPs films for the first electrode (**a**), second electrode (**b**), third electrode (**c**), and fourth electrode (**d**), respectively
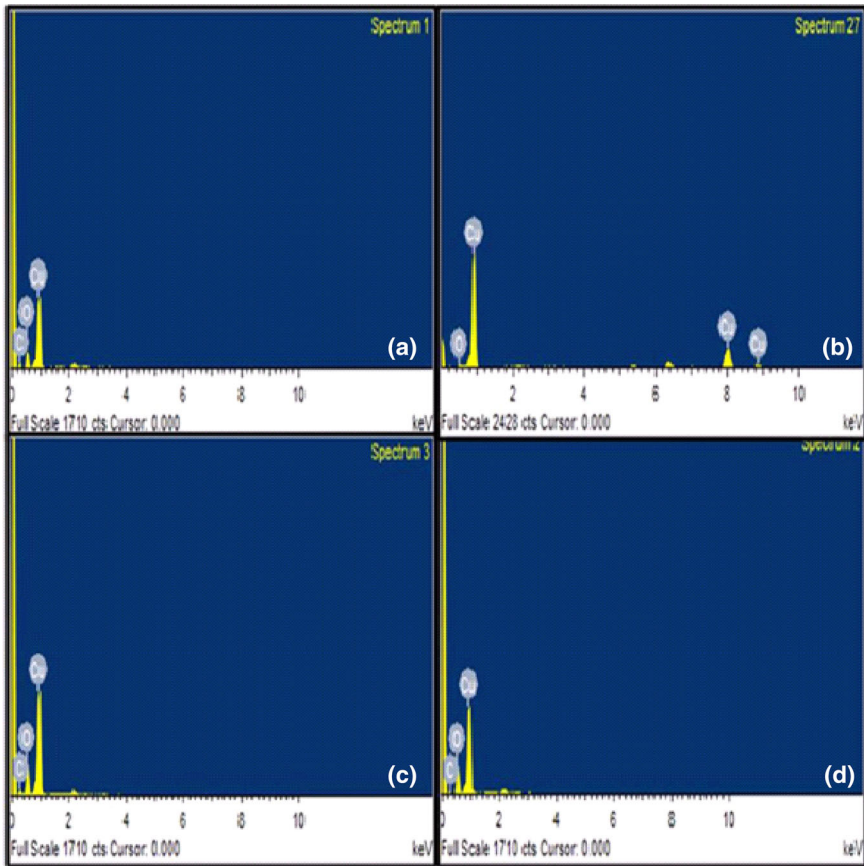
Fig. 3 EDS study of PPy/Cu NPs films for first electrode (**a**), second electrode (**b**), third electrode (**c**), and fourth electrode (**d**), respectively

Table 1 Elemental composition of PPy/Cu composite from EDS study

| Sr. no.	Element	Atomic (%)			
		First	Second	Third	Fourth
1	C	29.44	14.12	20.25	34.59
2	O	31.84	41.17	36.06	49.93
3	Cu	38.72	44.71	43.69	15.48
Total		100			

surface. As far as considering the third and fourth PPy/Cu films, the Cu nanoparticles agglomerate and start leaching from third to fourth PPy/Cu films; hence, it is clear from Table 1.

Electrocatalytic activity

To achieve optimal conditions for voltammetric determination of glucose, main parameters related to the film formation and solution characteristics were evaluated. Optimal conditions were explained by means of measuring the peak currents of both compounds with one variable at time method and determined as follows: 0.2 M pyrrole, 0.1 M NaOH, 10 cycles for electrodeposition of Cu nanoparticles, and pH 7.0 for electrolyte medium, respectively.

Without Cu NPs, bare PPy film (Fig. 4) shows no any oxidation or reduction peaks while applied for CV study in 10 mM glucose for different scan rates (10–50 mV s^{-1}). It reveals that PPy film shows very poor electrocatalytic activity. Hence, Cu NP decoration is needed to improve the electrocatalytic performance and in turns non-enzymatic glucose sensing of PPy/Cu NP electrode. Figure 5 shows the cyclic voltammograms recorded at PPy/Cu NPs on stainless steel substrate. Clear background signal was obtained in the absence of glucose (Fig. 5, black line) for the PPy electrode modified by Cu nanoparticles. Upon the addition of glucose of about 10 mM in the cell, oxidation and subsequent reduction peaks have appeared at − 0.6 and − 1.0 V, respectively, indicating a quasi-reversible electrode process probably due to the diffusion barrier of the polymeric film (Fig. 5, black and red lines, respectively).

The electrochemical reaction kinetics was improved as the copper nanoparticles were inserted to the polymeric film matrix by subsequent cycling of the potential in a range of − 0.6 and − 1.0 V. Therefore, PPy/Cu NPs/stainless steel has exhibited a large peak-to-peak separation with almost reversible electrochemical behaviour (E_p = 1.2 V). The peak currents have also increased 19 times studied in the presence of glucose. So far, the peak characteristics have clearly indicated an electrocatalytic oxidation of glucose at PPy-modified electrodes by the gain of a
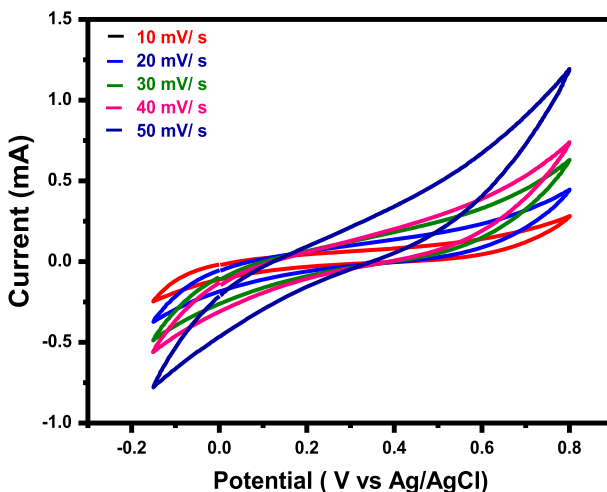
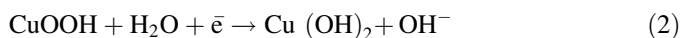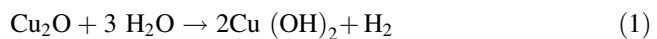**Fig. 4** Cyclic voltammetry (CV) study of bare PPy electrode in 10 mM glucose for scan rate 10–50 mV s^{-1}
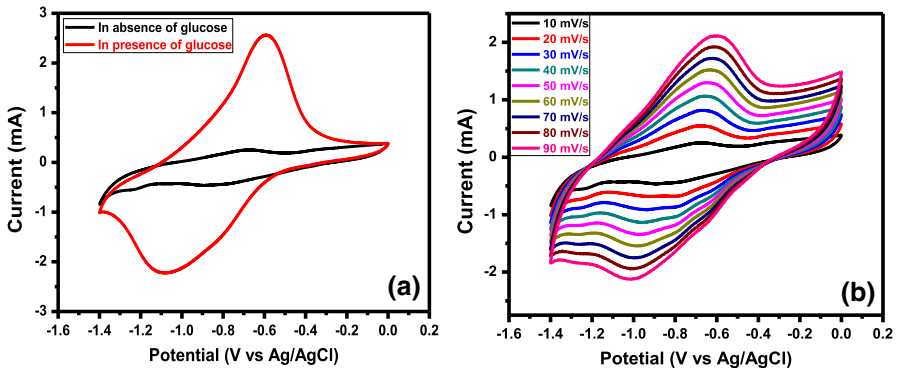
Fig. 5 CV study of PPy/Cu NPs films for in presence and in absence of glucose (**a**) and for different scan rates (**b**)

more active surface. The increase in the analytical determination sensitivity of glucose is a clear indication of the enlargement of active surface area of the PPy electrode modified by copper nanoparticles [38].
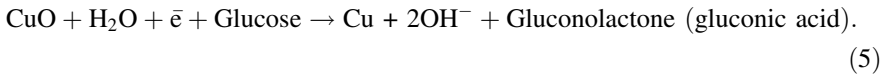
Cyclic voltammetry

The electrocatalytic activity of PPy/Cu NPs in the presence of 10 mM of glucose in 0.1 M NaOH solution for different scan rates (10–90 mV s^{-1}) was recorded. We were observed the enhancement in oxidation and reduction peak currents. Cu NPs acted as potential candidate during non-enzymatic glucose sensing due to its electrocatalytic properties, well-defined electrochemical redox activity, as shown in Fig. 5. Moreover, the increase of oxidation peak current and the shift of oxidation peak potential to higher voltage confirm the high sensitivity of the Cu-decorated PPy electrode for glucose detection [39]. The oxidation peak observed at 0.58 V and reduction peak at − 1.0 V is due to that it shows the formation of Cu (III)/Cu (II) couple peak redox reaction [40]. The production of Cu (III) is on the surface of Cu$_2$O thin film and glucose gets oxidized into gluconic acid. Cu (III) acts as a mediator for travel of electrons with catalytic activity. The cyclic voltammetry of Cu$_2$O thin films in the presence of 10 mM glucose in 0.1 M NaOH solution is shown in Fig. 5. The following reaction explains conversion of glucose-to-gluconic acid [41]. There are always the possible of dissolution, sintering, and agglomeration of metal-based catalysts during operation of catalytic reaction; hence, it is composed with PPy polymer applied as catalyst supports. Carbon-based electrodes provide a large electro active surface area and improve activity and durability of catalysts. The decoration of Cu NPs affects on the detection/sensing of glucose [42, 43]. Thus, the conversion of glucose to gluconolactone (gluconic acid) is explained as follows:

$$Cu_2O + 3 H_2O \rightarrow 2Cu (OH)_2 + H_2 \qquad (1)$$

$$CuOOH + H_2O + \bar{e} \rightarrow Cu (OH)_2 + OH^- \qquad (2)$$

$$Cu\,(OH)_2 \xrightarrow{\Delta} CuO + H_2O \tag{3}$$

$$CuO + H_2O + \bar{e} \rightarrow Cu + 2OH^- \tag{4}$$

Meanwhile, Cu nanoparticle which directly traduces glucose-to-gluconic acid by electrooxidation process. Electrooxidation of glucose on PPy/Cu NPs electrode surface is done by following equation:

$$CuO + H_2O + \bar{e} + Glucose \rightarrow Cu + 2OH^- + Gluconolactone\,(gluconic\;acid). \tag{5}$$

In the presence of 10 mM, glucose prepared in 0.1 M NaOH solution is used. It is clearly seen from Fig. 6a–d for different scan rates in 10 mM glucose for the
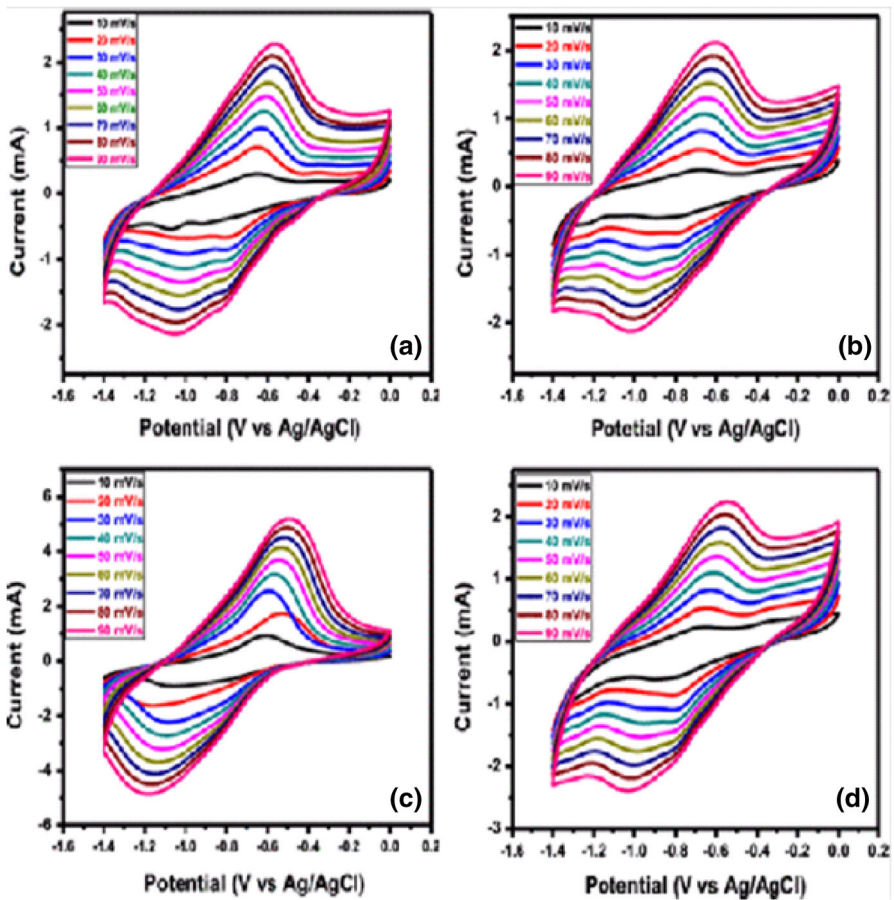

Fig. 6 Electrocatalytic activity of PPy/Cu NPs films using CV for different scan rates (10–90 mV s^{-1}) in 10 mM glucose for first electrode (**a**), second electrode (**b**), third electrode (**c**), and fourth electrode (**d**), respectively

first, second, third, and fourth films; cyclic voltammograms were help to investigate the electrocatalytic behaviour of PPy/Cu NPs. All CVs are measure for 10 mM glucose concentration in 0.1 M NaOH solution for different scan rates (10–90 mV s^{-1}). On the surfaces of PPy/Cu NP electrode, glucose is oxidized by various surface states of Cu through the transitions I–III [14, 17, 44]. The oxidation is mainly mediated by Cu (II)/Cu(III) transition to form gluconic acid and then to form format and carbonate through C–C bond cleavage which mentioned by some other group of researchers [14, 45]. Surface properties of the electrode play a major role in determining its electrochemical activity. (PPy) coated with Cu/Cu$_2$O surfaces can increase the conductivity and stability of the electrode and thus can decrease the over potential for glucose oxidation [15, 46, 47]. Glucose oxidation on Cu$_2$O/PPy electrodes in 0.1 M NaOH occurs in the potential range of − 1.6–0.2 V. PPy is assist to control Cu$_2$O structures mainly due to its greater electrochemical stability over applied potential window FE-SEM results also help to prove it [15].

Amperometric response of PPy/Cu NPs sensor

Figure 7 illustrates the amperometric response of PPy/Cu NPs for 10, 20, 30, and 40 mM glucose concentrations. As it is clearly observed from amperometric curve, we have taken the optimized film which is Cu nanoparticle which have been deposited by six cycles of cyclic voltammetry which is optimized film from cyclic voltammetry study of Fig. 6b. The current–time curves were recorded for optimized film. As the successive addition of glucose leads to increase in current, as shown in Fig. 7, the maximum current obtained 5.4 mA for 40 mM of glucose.
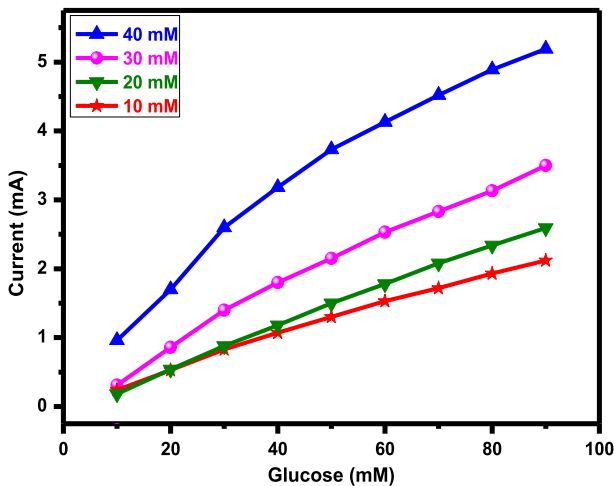
Fig. 7 Amperometric response of PPy/Cu NP films for the first, second, third, and fourth electrodes for 10, 20, 30, 40, and 50 mM glucose solution

Determination of glucose sensor

Detection limits for optimize film second in glucose were estimated to be 3.0 μM which comparatively less than rest of the first, third, and fourth films of LOD values 7.1, 5.28, and 11.4 μM. Figure 8 indicates linearity curve of optimized second electrode which shows stable peak observations at fixed concentration while increasing the glucose analyte concentration indicated that the oxidation of glucose by PPy/Cu NPs/stainless steel is relatively concentration independent. The sensitivity of PPy/Cu NPs/stainless steel electrode is calculated using formula slope/area of electrode. The sensitivity of PPy/Cu NPs/stainless steel electrode for the first, second, third, and fourth represented in Table 2. The optimum sensitivity of second electrode is 100 μA mM^{-1} cm^{-2} with LOD 3 μM and regression coefficient $R^2 = 0.9951$

Stability, repeatability, and reproducibility studies

The problem occurred in glucose detection for a PPy/Cu NPs non-enzymatic sensor is the electrochemical oxidation of meddling species such as fructose, lactose, and
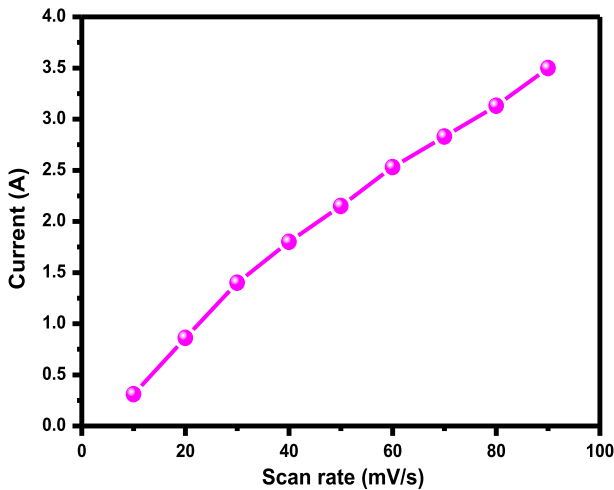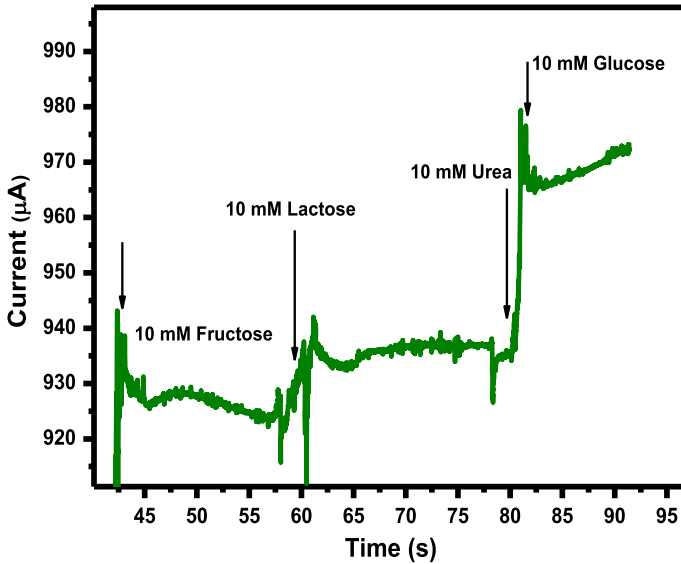

Fig. 8 Linearity curve of optimized second electrode

Table 2 Comparative study of sensing for all the synthesized electrodes

Sr. no.	Sensing parameters	Electrode used			
		First	Second	Third	Fourth
1	I_{max} (mA)	3.46	5.2	2.62	2.12
2	LOD (μM)	7.1	3	4.8	11.2
3	Sensitivity (μA mM^{-1} cm^{-2})	76	100	60	40

Fig. 9 Selectivity of PPy/Cu NP towards glucose

urea in physiological conditions. For selectivity of glucose, we should go for the amperometric study PPy/Cu NPs (Fig. 9) which reveal excellent selectivity towards glucose than lactose, fructose, and urea at potentials even 650 mV. Figure 9 shows the selective determination of glucose at the PPy/Cu NP electrode by successive addition of 0.1 mM fructose, 0.1 mM lactose, 0.1 mM urea, and 0.1 mM glucose to 0.1 M NaOH solution at an applied potential of 650 mV. The addition of lactose, fructose, and urea does not lead to any observable response or less than the response of glucose [39].

Figure 10 represents the stability curve of optimized PPy/Cu electrode of the proposed second electrode. Moreover, for glucose sensing, glucose was propped in air saturated PBS (pH 7.0), and its oxidation peak current response was monitored and registered periodically. The 74.27% of the initial oxidation peak current response remains withstand even after 10 days in the air at ambient temperature. It implies the unique stability of the reported second sensor for glucose. On the other hand, the reproducibility and repeatability of oxidation peak currents in the presence of glucose. In this context, relative standard deviation (RSD) was measured of about 4.16%, which indicates the better reproducibility and retaintivity of PPy/Cu electrode towards glucose sensing. The PPy/Cu non-enzymatic glucose sensor chose three individual as prepared modified electrodes and measured the corresponding. In present study, constructed PPy/Cu NP sensor shows very excellent performance in sensitivity, linear range, and selectivity. The results demonstrate that the PPy/Cu NP electrode is a promising candidate for non-enzymatic glucose determination
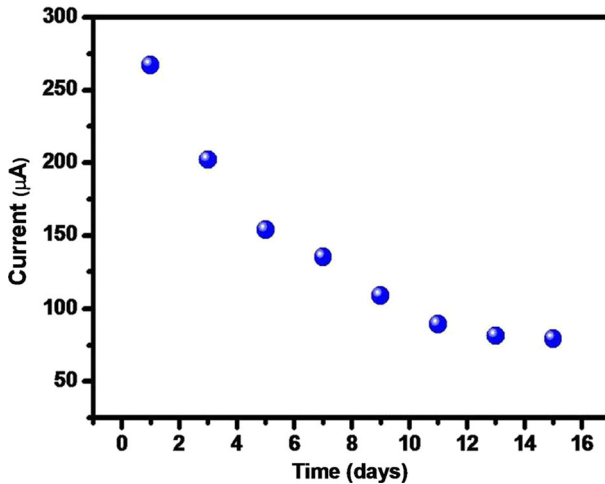
Fig. 10 Stability curve of second electrode

Conclusions

In the present study, a new composite electrode PPy/Cu NPs/stainless steel was prepared by electropolymerization and electrodeposition methods. It was shown that this composite electrode improved the electrocatalytic activities towards the oxidation of glucose. The catalytic activity of PPy/Cu NPs/stainless steel electrode towards glucose oxidation was improved by the formation of a uniform PPy film which was incorporated with Cu nanoparticles on the electrode surface due to the increasing effective surface area. The detection limits of glucose were estimated for the first, second, third, and fourth electrodes, 3 μM is optimized LOD for second film which also shows better amperometric response, respectively. Thus, the Cu nanoparticle-modified polypyrrole film electrode showed better sensitivity of $100\ \mu A\ \mu M^{-1}\ cm^{-2}$.

References

1. Meng F, Shi W, Sun Y, Zhu X, Wu G, Ruan C, Liu X, Ge D (2013) Nonenzymatic biosensor based on CuxO nanoparticles deposited on polypyrrole nanowires for improving detectionrange. Biosens Bioelectron 42:141–147
2. Malhotra BD, Chaubey A, Singh SP (2006) Prospects of conducting polymers in biosensors. Anal Chim Acta 578:59–74
3. Wang J (2008) Electrochemical glucose biosensors. Chem Rev 108:814–825
4. Fiorito PA, Brett CMA, Torresi SC (2006) Polypyrrole/copper hexacyanoferrate hybrid as redox mediator for glucose biosensors. Talanta 69:403–408
5. Yi X, Huang-Xian J, Hong-Yuan C (2000) Direct electrochemistry of horseradish peroxidase immobilized on a colloid/cysteamine-modified gold electrode. Anal Biochem 278:22–28
6. Zhang J, Oyama M (2004) A hydrogen peroxide sensor based on the peroxidase activity of hemoglobin immobilized on gold nanoparticles-modified ITO electrode. Electrochim Acta 50:85–90

7. Strike DJ, Rooij NFD, Koudelka-Hep M, Ulmann M, Augustynski J (1992) Electrocatalytic oxidation of methanol on platinum microparticles in polypyrrole. Appl Electrochem 22:922–926

8. Rau JR, Chen SC, Sun HW (1994) Characterization of a polypyrrole microsensor for nitrate and nitrite ions. Electrochim Acta 39:2773–2779

9. Li J, Lin XQ (2007) Glucose biosensor based on immobilization of glucose oxidase in poly(o-aminophenol) film on polypyrrole-Pt nanocomposite modified glassy carbon electrode. Biosens Bioelectron 22:2898–2905

10. Bose CSC, Rajeshwar K (1992) Efficient electrocatalyst assemblies for proton and oxygen reduction: the electrosynthesis and characterization of polypyrrole films containing nanodispersed platinum particles. Electroanal Chem 333:235–256

11. Chen W, Li CM (2007) Electrosynthesis and characterization of polypyrrole/Au nanocomposite. Electrochim Acta 52:2845-2849

12. Roux S, Soler-Illia GJ, Champagne S, Audebert P, Sanchez C (2003) Titania/polypyrrole hybrid nanocomposites built from in-situ generated organically functionalized nanoanatase building blocks. Adv Mater 15:217–221

13. Liu YC, Lee HT, Yang SJ (2006) Strategy for the syntheses of isolated fine silver nanoparticles and polypyrrole/silver nanocomposites on gold substrates. Electrochim Acta 51:3441–3445

14. Ozcan L, Sahin M, Sahin Y (2008) Electrochemical preparation of a molecularly imprinted poly-pyrrole-modified pencil graphite electrode for determination of ascorbic acid. Sensors 8:5792–5805

15. Ozkorucuklu S, Sahin Y, Alsancak G (2008) Voltammetric behaviour of sulfamethoxazole on electropolymerized-molecularly imprinted overoxidized polypyrrole. Sensors 8:8463–8478

16. Wang L, Ma C, Zhang X, Ren Y, Yu Y (1995) Determination of tyrosine traces by adsorption voltammetry of its copper (II) complex. J Anal Chem 351:689–691

17. Liu L, Zhao F, Xio F, Zeng B (2008) Improved voltammetric response of L-tyrosine on multiwalled carbon nanotubes-ionic liquid composite coated glassy electrodes in the presence of cupric ion. Electroanalysis 20:2148–2152

18. Liu K, Li Y, Zhang H, Liu Y (2018) Synthesis of the polypyrrole encapsulated copper nanowires with excellent oxidation resistance and temporal stability. Appl Surf Sci 439:226–231

19. Aravindan N, Sangaranarayanan MV (2016) Influence of solvent composition on the anti-corrosion performance of copper–polypyrrole (Cu–PPy) coated 304 stainless steel. Prog Org Coat 95:38–45

20. He X, Chen Y, Wang S, He W, Wang C, Zhang H, Li Q, Ai K (2018) Enhancing inductance of spiral copper inductor with BaFe₁₂O₁₉/poly (phenylene oxide) composite as an embedded magnetic core. Compos B 138:232–242

21. Arena A, Scandurra G, Ciofi C (2017) Copper oxide chitosan nanocomposite: characterization and application in non-enzymatic hydrogen peroxide sensing. Sensors 17:2198–2209

22. Qing L, Zhang B, Xing X, Zhao Y, Cai R, Wang W, Gu Q (2018) Biosynthesis of copper nanoparticles using Shewanella loihica PV-4 with antibacterial activity: novel approach and mechanisms investigation. J Hazard Mater 347:141–149

23. Liang J, Wei M, Wang Q, Zhao Z, Liu A, Yu Z, Tian Y (2018) Sensitive electrochemical determination of hydrogen peroxide using copper nanoparticles in a polyaniline film on a glassy carbon electrode. Anal Lett 51:512–522

24. Kaviyarasan K, Anandan S, Mangalaraja RV, Sivasankar T, Ashokkumar M (2016) Sonochemical synthesis of Cu₂O nanocubes for enhanced chemiluminescence applications. Ultrason Sonochem 29:388–393

25. Chen LY, Wang CW, Yuan Z, Chang HT (2014) Fluorescent gold nanoclusters: recent advances in sensing and imaging. Anal Chem 87:216–229

26. Chen PC, Roy P, Chen LY, Ravindranath R, Chang HT (2014) Gold and silver nanomaterial-based optical sensing systems. Part Part Syst Char 31:917–942

27. Heller A, Feldman B (2008) Electrochemical glucose sensors and their applications in diabetes management. Chem Rev 108:2482–2505

28. Periasamy AP, Chang Y-J, Chen S-M (2011) Amperometric glucose sensor-based on glucose oxidase immobilised on geletin-multiwalled carbon nanotube modified glassy carbon electrode. Bioelectrochemistry 80:114–120

29. Roy P, Lin ZH, Liang CT, Chang HT (2012) Synthesis of enzyme mimics of iron telluride nanorods for the detection of glucose. Chem Commun 48:4079–4081

30. Shiang YC, Huang CC, Chang HT (2009) Gold nanodot-based luminescent sensor for the detection of hydrogen peroxide and glucose. Chem Commun 23:3437–3439

31. Yeh TY, Wang CI, Chang HT (2013) Photoluminescent C-dots@RGO for sensitive detection of hydrogen peroxide and glucose. Talanta 115:718–723
32. Mani V, Devadas B, Chen SM (2013) Direct electrochemistry of glucose oxidase at electrochemically reduced graphene oxide-multiwalled carbon nanotubes hybrid material modified electrode for glucose biosensor. Biosens Bioelectron 41:309–315
33. Park S, Boo H, Chung TD (2006) Electrochemical non-enzymatic glucose sensors. Anal Chim Acta 556:46–57
34. Wei H, Wang E (2013) Nanomaterials with enzyme-like characteristics (nanozymes): next-generation artificial enzymes. Chem Soc Rev 42:6060–6093
35. Leskovac V, Trivi S, Wohlfahrt G, Kandra J, Pericin D (2005) Glucose oxidase from *Aspergillus niger*: the mechanism of action with molecular oxygen, quinones, and one-electron acceptors. Int J Biochem Cell Biol 37:731–750
36. Rabiee M, Mirzadeh H, Ataie Jr A (2016) Unraveling the effects of process control agents on mechanical alloying of nanostructured Cu-Fe alloy. Ultrafine Grained Nanostruct Mater 49:17–21
37. Chokratanasombat P, Nisaratanporn E (2012) Preparation of ultrafine copper powders with controllable size via polyol process with sodium hydroxide addition. Eng J 16:40–46
38. Ulubay S, Dursun Z (2010) Cu nanoparticles incorporated polypyrrole modified GCE for sensitive simultaneous determination of dopamine and uric acid. Talanta 80:1461–1466
39. Shackerya I, Patila U, Pezeshkib A, Shinde NM, Kanga S, Imb S, Juna SC (2016) Copper hydroxide nanorods decorated porous graphene foam electrodes for non-enzymatic glucose sensing. Electrochim Acta 191:954–961
40. Lu N, Shao C, Li X, Shen T, Zhang M, Miao F, Zhang P, Zhang X, Wang K, Zhang Y, Liu Y (2014) CuO/Cu$_2$O nanofibers as electrode materials for non-enzymatic glucose sensors with improved sensitivity. RSC Adv 4:31056–31061
41. Khan R, Ahmad R, Rai P, Jang LW, Yun JH, Hahn YB, Lee IH (2014) Glucose-assisted synthesis of Cu$_2$O shuriken-like nanostructures and their application as nonenzymatic glucose biosensors. Sens Actuators B 203:471–476
42. Li Z, Ye C, Li X, Ding Y, Liang H, Zhao G, Wang Y (2018) A CuNi/C nanosheet array based on a metal–organic framework derivate as a supersensitive non-enzymatic glucose sensor. Nano-Micro Lett 10:28–38
43. Pagare PK, Torane AP (2016) Band gap varied cuprous oxide (Cu$_2$O) thin films as a tool for glucose sensing. Microchim Acta 183:2983–2989
44. Li C (2006) Voltammetric determination of tyrosine based on an l-serine polymer film electrode. Colloid Surf B 50:147–151
45. Alexander C, Andersson HS, Andersson LI, Ansell RJ, Kirsch N, Nicholls IA, O'Mahony J, Whitcombe MJ (2006) Molecular imprinting science and technology: a survey of the literature for the years up to and including 2003. J Mol Recogn 19:106–180
46. Pardieu E, Cheap H, Vedrine C, Lazerges M, Lattach Y, Garnier F, Remita S, Pernelle C (2009) Molecularly imprinted conducting polymer based electrochemical sensor for detection of atrazine. Anal Chim Acta 649:236–245
47. Wen-Zhi L, You-Qin L (2009) Preparation of nano-copper oxide modified glassy carbon electrode by a novel film plating/potential cycling method and its characterization. Sens Actuators B 141:147–153